A R C H I V E S O F M E T A L L U R G Y A N D M A T E R I A L S
Volume 58 2013 Issue 2
DOI: 10.2478/amm-2013-0005

A. KRUK*, A. CZYRSKA-FILEMONOWICZ*

CONTRIBUTION OF ELECTRON TOMOGRAPHY TO DEVELOPMENT OF INNOVATIVE MATERIALS FOR CLEAN ENERGY SYSTEMS AND AERONAUTICS

WKŁAD TOMOGRAFII ELEKTRONOWEJ DO ROZWOJU INNOWACYJNYCH MATERIAŁÓW DLA NISKOEMISYJNYCH SYSTEMÓW ENERGETYCZNYCH I LOTNICTWA

The development of innovative materials for clean energy systems and aeronautics requires use of modern research methods to characterize the structure on the level from micro- to nanoscale. Modern two-dimensional imaging techniques recently available in electron microscopes allow use of tomographic methods to characterize the structure of materials. Application of modern three dimensional imaging techniques such as electron tomography allows accurate qualitative and quantitative measurement of the structure elements in the micro- and nanoscale. The electron tomography studies have been carried out for three-dimensional visualization and metrology of different materials for clean energy systems and aeronautics. Electron tomography results provided quantitative data about shape, size and distribution of the particles, complementary to those obtained by means of quantitative TEM metallography.

Keywords: TEM, STEM-HAADF, EFTEM, FIB-SEM, tomography

Rozwój innowacyjnych materiałów dla niskoemisyjnych systemów energetycznych i lotnictwa wymaga zastosowania nowoczesnych metod badawczych w celu scharakteryzowania struktury na poziomie od mikro- do nanoskali. Nowoczesne dwuwymiarowe techniki obrazowania od niedawna dostępne w mikroskopach elektronowych, umożliwiają zastosowanie metod tomograficznych do scharakteryzowania struktury materiałów. Zastosowanie nowoczesnych technik trójwymiarowego obrazowania, takich jak tomografia elektronowa umożliwia dokładny jakościowy i ilościowy pomiar elementów mikrostruktury w mikro- i nanoskali. Badania metodami tomografii elektronowej przeprowadzone zostały w celu trójwymiarowej wizualizacji i metrologii elementów mikrostruktury różnych materiałów konstrukcyjnych dla systemów niskoemisyjnej energetyki i lotnictwa. Badania metodami tomografii elektronowej dostarczają danych ilościowych dotyczących kształtów, wielkości i rozkładu przestrzennego cząstek i są one uzupełnieniem do danych uzyskiwanych za pomocą metod ilościowej analizy metalograficznej przy wykorzystaniu transmisyjnej mikroskopii elektronowej.

1. Introduction

The development of innovative materials for clean energy systems and aeronautics requires use of modern research methods to characterize the structure on the level from micro- to nanoscale. Modern 2D imaging techniques recently available in electron microscopes allow use of tomographic methods to characterize the structure of materials [1, 2]. Application of these methods enables to estimate the influence of the structural parameters on mechanical and corrosion properties of modern structural materials with high accuracy. Transmission- and Scanning Electron Microscopy (TEM, SEM) methods provide the qualitative and quantitative information about the phase composition and morphology engineering materials. However, most of them are based on metrology of the 2D projections of the 3D objects. Application of new (in material science) electron tomography techniques, such as TEM and Focused Ion Beam Scanning Electron Microscopy (FIB-SEM) tomography, gives the new opportunities. Those techniques allow us to reconstruct the microstructure of investigated materials in three dimensions. TEM images give valuable information about the microstructure and chemical composition of materials. However, they "only" provide a 2D projection of a 3D object. Electron tomography was developed to reconstruct objects in three dimensions (3D) from a tilt series of TEM or SEM images. This technique is well accepted in the life sciences as a method used to study viruses or cells [3]. The resolution in the reconstructions, however, is limited to a few nanometers. Electron tomography techniques have recently been adopted by researchers to materials science [4-6]. In practice, the resolution is still in the order of one to two nanometers because of the limited stability of the sample holders and the presence of dynamic diffraction in crystalline solids.

Electron tomography is a technique that uses the TEM or SEM to determine a 3D structure from any given asymmetric

* AGH UNIVERSITY OF SCIENCE AND TECHNOLOGY, INTERNATIONAL CENTRE OF ELECTRON MICROSCOPY FOR MATERIALS SCIENCE & FACULTY OF METALS ENGINEERING AND INDUSTRIAL COMPUTER SCIENCE, AL. A. MICKIEWICZA 30, 30-059 KRAKÓW, POLAND

object [4]. This process can be simply divided into four steps. First, a series of 2D projection images of the specimen are recorded semi automatically and systematically tilted to different angles in the microscope. During registration a series of images shift adjustment is performed between subsequent images. In second step, these individual images are aligned to a common origin. In the next step, the projections are reconstructed using for example Backprojected method (BP) to create a 3D representation of the sample in the Fourier space. The Direct Fourier Method (BP) and the Filtered Backprojection method (WBP) are two of the most well-known heuristics for tomographic reconstruction. The last step is connected with 3D visualization and metrology of reconstructed object.

A requirement for the calculation of 3D reconstructions from electron micrographs in electron tomography is that the registered image contrast must be a projection of some physical characteristic of the sample, e.g. its mass/electron density (Z-contrast) [3]. This implies that besides conventional TEM bright-field (TEM-BF) imaging, dominated by diffraction and/or scattering contrast, several different modes of image acquisition can be utilized in electron tomography to give insight into different characteristics of the sample [4]. Energy filtered transmission electron microscopy (EFTEM) and X-ray spectroscopic imaging (STEM-EDX), for instance, enable the mapping of local concentrations of selected chemical elements. In EFTEM technique signal-to-noise ratios (SNR) are poor and every element map requires the registration of multiple images in each projection, which is disadvantageous if beam-sensitive samples are investigated. On the other hand, certain other acquisition modes are unsuitable (e.g. images based on Bragg angle diffraction contrast). In this case, however, the problem can be overcome by acquiring projection images with high angular annular dark-field scanning transmission electron microscopy (STEM-HAADF) utilizing Z-contrast [4]. Although these methods are very powerful, exposure (scanning) times of 10÷30 sec. per image are required when using STEM-HAADF and, furthermore, scanning noise cannot be avoided.

The Focused Ion Beam (FIB) has become an important tool in materials science for studying of materials at the micro- and nanometer scale [5-8]. FIB-SEM tomography is based on a serial slicing technique employing a FIB-SEM dual beam workstation. In the studies described below, electron tomography images were recorded by dual beam workstation (Zeiss NEON 40EsB CrossBeam) equipped with a FIB column (Ga^+ ions). The experimental details are given elsewhere [1]. Dual-beam SEM enables the acquisition of serial images with small (few nanometres) and reproducible spacing between the single imaging planes. No mechanical stage tilting is necessary between the FIB milling and the electron beam SEM imaging steps. Serial FIB cross-sections are performed through the investigated volume and each exposed surface is imaged with a scanning electron microscope. With application of computer algorithms for experimental data processing and graphics packages for 3D visualization can be easily reconstructed and the microstructure interrogated to obtain both qualitative and quantitative information. It is possible to study features at spatial resolutions at the level of tens of nanometers and volumes up to tens of cube microns.

In the studies presented below the STEM-HAADF, EFTEM, STEM-EDX tomography and FIB-SEM tomography have been carried out to visualize three-dimensional morphology of different materials: ferritic ODS alloy INCOLOY MA956 (oxide dispersoids), IN 718 and CMSX-4 Ni-base superalloys (3D distribution of nanoparticles), W-based alloys for fusion applications (distribution of carbides and porosity), low-alloyed creep-resistant Cr-V-Mo bainitic steel (carbides distribution). Electron tomography results provided quantitative data about shape, size and distribution the microstructural elements, complementary to those obtained by means of quantitative TEM metallography. Obtained results showed that FIB-SEM, a meso-scale tomography technique, is suitable for 3D reconstruction of the objects of 100 nm in size or even smaller.

2. Application of EFTEM and FIB-SEM electron tomography to 3D visualization and metrology of nanoparticles in Inconel 718 superalloy

Inconel 718 (IN 718) is a commercial nickel-base superalloy, used in aeronautics, space and nuclear industry, e.g. for critical pieces in gas turbine engines, rocket motors and nuclear reactors. Chemical composition of the IN 718 is as follows (wt %): Ni -19Fe -18Cr -5Nb -3Mo -1Ti -0.5Al - 0.04 C. Its microstructure consists of a γ matrix (Ni-based solid solution) containing the γ' (Ni_3Al) and γ" (Ni_3Nb) coherent nanoparticles. The primary strengthening mechanism for this alloy is a precipitation hardening by the γ' and γ" particles and therefore properly sized and distributed precipitates are critical for good alloy performance [9]. For electron tomography investigation the samples of IN 718 were prepared in the form of electrochemically polished thin foils. Tilt series were acquired semi automatically using Tecnai G2 microscope operating at 200 kV with use of FEI Xplore 3D software. Although titanium partitions to both γ' and γ" phases, the Ti maps were not collected in wide tilt angles, because the EFTEM images provided by the Ti $L_{2,3}$ at 455.5 eV exhibited low signal-to-noise ratio (SNR) compared with the Cr maps. Figure 1 shows the examples of the EFTEM maps of chromium, contained in γ phase, in different tilt angles from –43° to +52.5°. The EFTEM images were collected in Cr $L_{2,3}$ edges at 574 eV, which were well visible in EELS spectra. Taking into account that the γ matrix is rich in chromium and good quality of the EFTEM Cr mapping, it was more suitable to analyze the shape of the precipitates from a tomographic reconstruction of a tilt series of the absence of chromium. Tomographic reconstruction result is shown in Fig. 2.

Additionally, FIB-SEM tomography technique was used for imaging, characterization and metrology of strengthening particles in IN 718 alloy. Repeated removal of layers as thin as several nm for some hundred times permits to investigate at total a volume of some nm^3 with a voxel size as 2.5 nm×2.5 nm×2.5 nm. The 3D mapping of nanoparticles with high resolution by serial FIB slicing (in a distance of about 2.5 nm) and SEM imaging was performed. Ga ion beam at 30 kV was used to perform a precise in-situ milling. The SEM images at accelerating voltage 1.5 kV were taken with using BSE (Back Scattered Electron) detector. To visualize the 3D

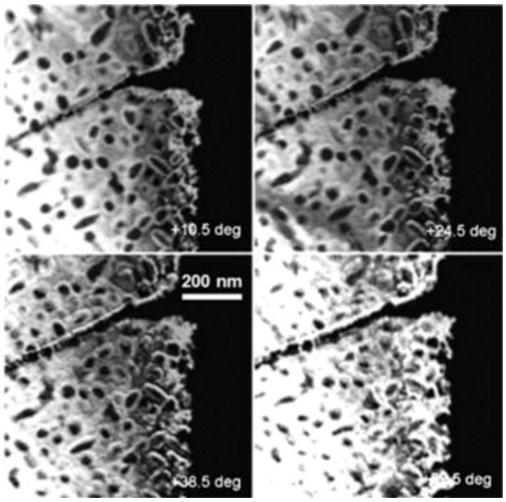

Fig. 1. Example of four Cr EFTEM elemental maps (slices) from the raw data stack of IN 718 alloy (tilt range of −45° to +60° with a 4° step)

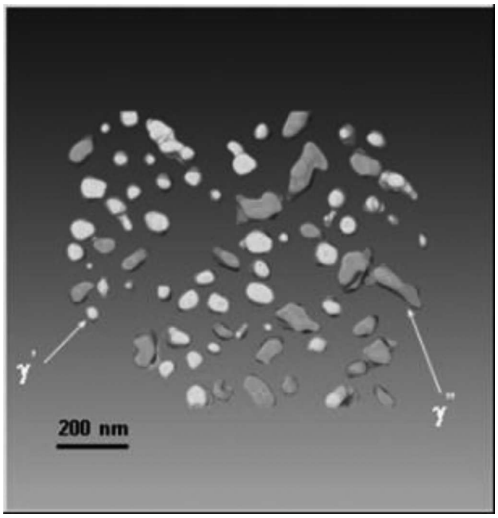

Fig. 2. Orthogonal view of the 3D surface rendering from the SIRT reconstructions for γ' (yellow) and γ'' (orange) nanoparticles in IN 718

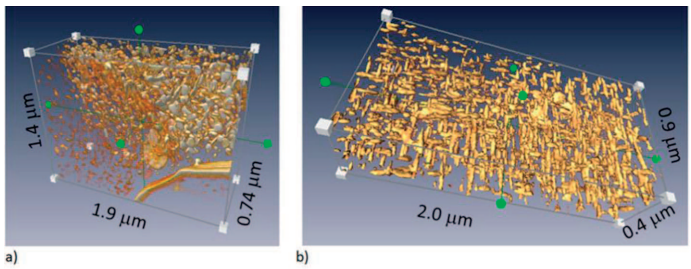

Fig. 3. Three-dimensional imaging of γ' and γ'' nanoparticles in IN 718 superalloy using FIB-SEM tomography. 3D visualization of FIB serial slicing and SEM imaging stack, voxel size in the raw data volume is 3×3×5 nm. Reconstructed volume: a) 1.9×1.4×0.74 μm, b) 2.0×0.9×0.4 μm

reconstruction, the Amira 5.4.1 and ImageJA 1.45b software were used. Filtering and shift correction performed on the images using cross-correlation method allowed for 3D visualization of the reconstructed volume. The image processing and segmentation permitted on the quantitative evaluation of the microstructure components. The volume fraction V_v of γ'' precipitates is equal 6.27±2.4% and the mean volume of the precipitates V_{ave} = $22.17 \cdot 10^3 \pm 9.7 \cdot 10^3$ nm^3. Figure 3 presents an example of visualization in 3D of a reconstructed sample volume. The results achieved for γ' and γ'' precipitates in IN 718 superalloy confirm the ability of FIB-SEM tomography to reconstruct 3D structures with dimensions in the range of 100 nm or even smaller. Such 3D reconstructions can serve as a basis for quantitative analysis of complex structures in a nanoscale.

3. Three-dimensional imaging of grains, porosity and TiC particles in tungsten-base alloy for fusion reactors using FIB-SEM tomography

Tungsten and its alloys are considered as potential candidates for plasma facing materials, particularly in the divertor and the first wall in nuclear fusion reactor due to the low sputtering rate, high thermal conductivity, high strength at elevated temperatures and low tritium inventory [10]. Previously described FIB-SEM tomography technique was used for study of microstructural features of W-1.7 % TiC alloy in three dimensions. The SEM images were acquired with use of BSE detector. The distance between slices was about 5 nm. Consequently, the acquired stack of images can be transformed directly into a 3D data volume with a voxel resolution of 3.8×3.8×5 nm. Filtering and shift correction performed on the images using cross-correlation method allowed for 3D visualization of the reconstructed volume.

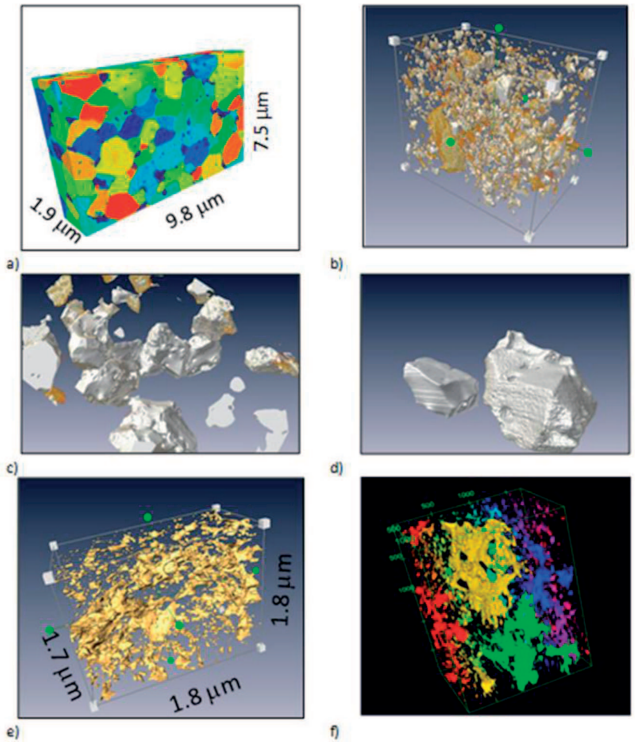

Fig. 4. Three-dimensional characterization of W-1.7%TiC alloy microstructure using FIB-SEM tomography: a) microstructure of W-1.7%TiC alloy as seen by SEM-BSE imaging, b) 3D visualization of pores and particles, c, d) visualization of grains, e) 3D visualization of pores and particles, f) 3D visualization of reconstructed volume, varied in respect of the pore dimension are labeled with a different color levels. Voxel size in the raw data volume is 3.8×3.8×5 nm

Three-dimensional visualization of pores and cracks in tungsten-base alloy is presented in Fig. 4. The reconstructed volume was 4.21×3.7×0.3 μm^3. The pores can be divided into large irregular and small oval in shape, marked in different colors, respectively. Such 3D imaging gives the qualitative information about size, shape and spatial distribution of pores. The relative volume of pores and particles in this volume was estimated to be 5.19±1.35%. Mean diameter of particles in that volume was estimated as 32.6±18.8 nm.

4. Three-dimensional imaging of the carbides in Cr-V-Mo steel using FIB-SEM and STEM-HAADF tomography

Low alloyed Cr-Mo-V (13HMF) steels are extensively used for various engineering components in thermal power plants. In the heat and power generating plants, the pipelines are used to transport superheated steam in the temperature range 500-560°C and under a pressure of 10-15 MPa. This steel should retain a stable microstructure during long time operation at elevated temperature to ensure good mechanical properties. However during long term service in such conditions, the steel changes its microstructure due to creep deformation; pearlite/bainite decomposes as well as carbides precipitation at the grain boundaries and carbides coarsening processes proceed [11]. Electron tomography, was used for detailed characterisation and metrology of carbides in 0.5%Cr-0.5%Mo-0.25%V low alloy steel after service at 540 °C for 160 000 h. For FIB-SEM tomography investigation, serial FIB cross-sections are performed through the volume to be investigated and each exposed surface is imaged with the SEM. The 3D mapping of the particles with high resolution by serial FIB slicing and SEM imaging was performed. Ga-ion beam at parameters: 30 kV, 100 pA and aperture of 30 μm was used to perform a precise in-situ milling. The SEM images (image size: 530×461 pixels, 8bit grayscale) using low voltage of 1.7 kV in SEM mode were taken with use of BSE detector. Repeated removal of layers as thin as a 5 nm allows to explore at total a volume of some 7.9×3.6×1.2 μm with the voxel size 5×5×5 nm (size of raw data stack: 375 MB). The 3D visualization of reconstructed space for FIB-SEM tomography was performed using ImageJA 1.45b and Amira 5.4.1. The different shapes and spatial distribution of carbide particles in reconstructed volume are shown in Fig.5. The estimated mean particle volume of Mo_2C is $12.5 \cdot 10^3 \pm 6.9 \cdot 10^3$ nm^3.

The samples for electron tomography were prepared in the form of extraction double replicas. In our investigations tilt series were acquired semi automatically using Tecnai G2 microscope. Digital images were recorded with a 1K Gatan 794 slow scan CCD camera in a tilt range from –74° to +74° at intervals of 2°. The tomograms were generated using Xplore 3D software. All tilted images were aligned to a common tilt axis using cross-correlation and the volume was reconstructed using WBP method. The 3D visualization of reconstructed space was performed using Amira 5.4.1 software. In spite of the exact shift correction of the object in relation to the rotation axis, the effect of visualization is not ideal (Fig. 6). The improvement of the reconstruction image quality can be obtained by using the iterative methods (ART, SIRT) in reconstruction.

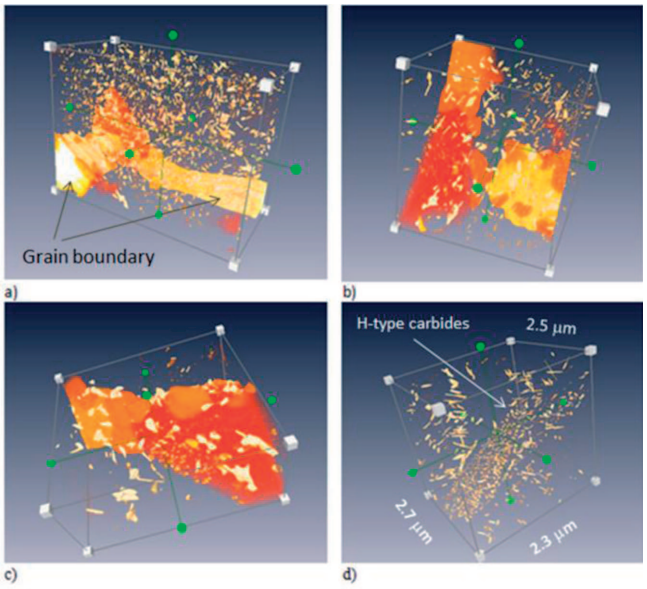

Fig. 5. Three-dimensional visualisation of spatial shape of carbides in the 13HMF steel. Voxel size in the raw data volume is 5×5×5 nm. a) 3D visualization of reconstructed volume: 5.12×3.84 ×2.5 μm, b, c) reconstructed volume 2.7×2.3×2.5 μm, d) spatial distribution of H-type carbides precipitates on the ferrite sub-grain boundary

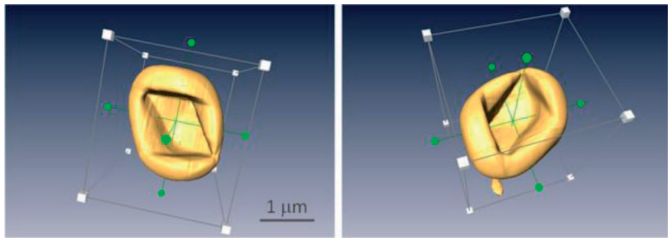

Fig. 6. 3D visualization of Ti(C,N) particle

5. Application of STEM-HAADF and FIB-SEM tomography to 3D visualization of oxide dispersoids in INCOLOY MA956

Incoloy MA956 is a mechanically alloyed Oxide Dispersion Strengthened (ODS) alloy, which combines a high temperature creep and oxidation resistance due to the incorporation of Y-Al oxide nanoparticles in a ferritic FeCrAl matrix. The nominal chemical composition is as follows (in wt %): Fe - 20Cr - 4.5Al - 0.5 Ti - 0.5 Y_2O_3 [12]. Application of electron tomography techniques gives the possibility to reconstruct the oxide dispersoids in three dimensions (3D). The sample was prepared as an extraction double replica. The Y-Al dispersoids were extracted from the Incoloy MA956 after isothermal annealing at 1350°C for 1000 hours. Tilt series in STEM-HAADF mode were acquired semi- automatically using FEI Xplore 3D software with a tilt range of −74° to +74° with a 2° step, than aligned and reconstructed using a WBP algorithm in the FEI Inspect3D software. However due to the limited tilt range and a small number of projections, the missing information should be encountered in interpretation of results. Considering the missing wedge of information it was not possible to perform shape analysis of oxide nanoparticles

with the required resolution to determine facets or planes of each particle.

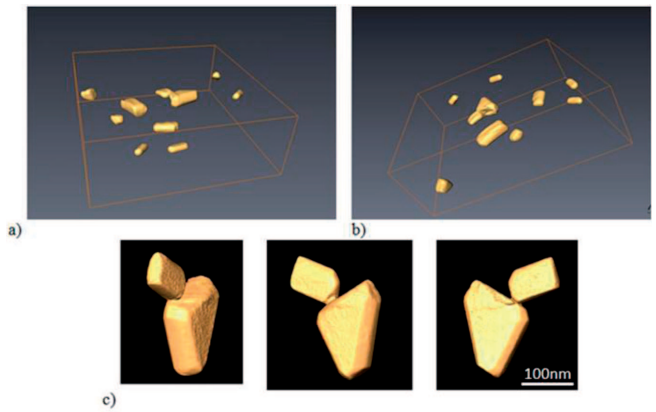

Fig. 7. a, b) 3D visualization of Y-Al oxide dispersoids in reconstructed volume of Incoloy MA956, spatial distribution of dispersoids in reconstructed volume, c) complex particle at different angles of view

For FIB-SEM tomography of the SEM images (image size: 996×455 pixels, 8bit gray-scale) were taken using in-lens SE detector at low voltage of 1.7 kV. The distance between slices was about 8 nm. Repeated removal of layers as thin as a 8 nm allowed to explore a total volume of 7.9×3.6×1.2 μm with the voxel size 8×8×8 nm (size of raw data stack: 62 MB). The shape and dimensions of selected oxides particle is illustrated in Fig. 8. The volume fraction of oxide particles presented in reconstructed volume was measured as $V_v = 0.62\pm0.1\%$. The mean particle volume is $V_{ave} = 5.34\cdot10^5\pm5.27\cdot10^5$ nm^3. Thus, the mean equivalent sphere diameter of the Y-Al oxides is $d_{eq} = 92.3\pm28.7$ nm.

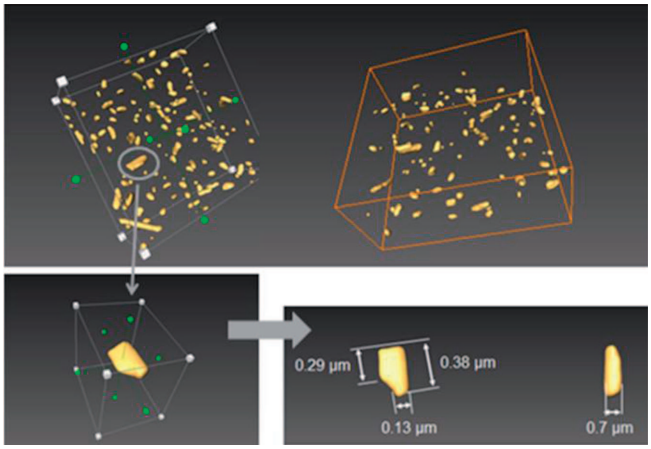

Fig. 8. The 3D visualization of Y-Al oxide particles in reconstructed volume 3.6×2.0×1.2 μm and metrology of single particle in Incoloy MA956 by electron tomography. Volume fraction of oxide particles, $V_v = 0.62\pm0.1\%$

6. The 3D imaging and metrology of Ni-base CMSX-4 superalloy microstructure using FIB-SEM and STEM-EDX tomography methods

The single crystal nickel-base CMSX-4 superalloy is widely used for gas turbine blades of aeroengines as well as in power generation plants. Its microstructure is especially tailored to ensure the high microstructure stability and the high temperature strength by the absence of grain boundaries, strengthening by high volume fraction of cuboidal intermetallic γ' precipitates and nanometric width of γ matrix channels. The qualitative and quantitative microstructural analysis of CMXS-4 ex-service turbine blade after operation for 12 700 hours and 200 starts in industrial gas turbine were performed using FIB-SEM and STEM-EDX tomographic methods. The distribution of temperature and stress in the analysed regions of blade was as follows: 927°C/111 MPa at the middle of the blade height, 807°C/189 MPa at the blade bottom [13].

FIB-SEM tomography was carried out using a serial slicing technique employing a FIB-SEM dual beam workstation as described in Chapter 1. The distance between slices was about 8 nm. Consequently, the acquired stack of images was transformed directly into a 3D data volume with a voxel resolution of 8×8×8 nm. Figure 9 shows the 3D visualization of the γ and γ' in CMSX-4 superalloy after image filtering and shift correction.

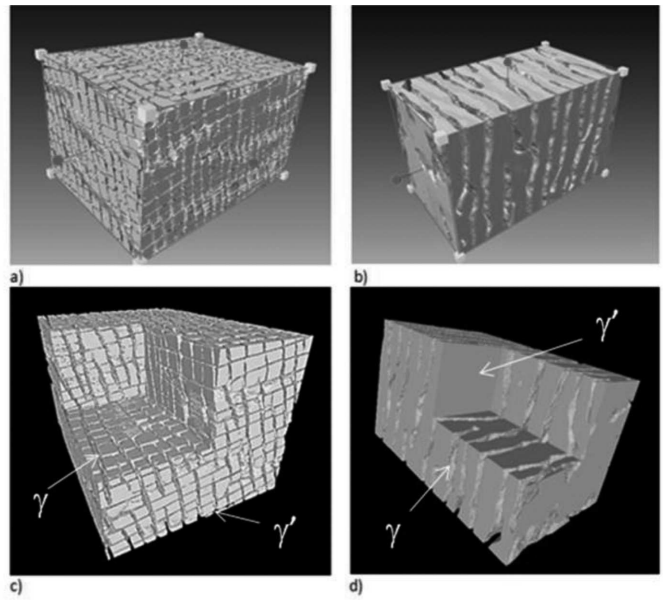

Fig. 9. 3D visualization of γ and γ' phases in reconstructed volume 7.7×4.4×3.5 μm in ex-service turbine blade of CMSX-4 superalloy, voxel size 8×8×8 nm, a, c) shape and spatial distribution of γ' particles and γ channels at the blade bottom (807°C/189 MPa), b, d) at the middle of the blade height (927°C/111 MPa)

The other method used for imaging of 3D microstructure of the CMSX-4 superalloy was STEM-EDX tomography. Application of probe Cs corrected Titan Cubed G2 60-300 with EDX ChemiSTEM^{TM}technology allowed to achieve high X-ray signal over a large tilt angle of investigated sample and collect a tomographic series of 2D elemental maps in the angular range from -40° to +60° with step of 5°. Tomographic reconstruction of a tilt series images was performed using ART method, which allowed visualizing the three-dimensional distribution of element in the analysed volume. STEM-EDX elemental Cr map images at -40°, 0° and 60° tilt angle, selected from the registered tilt series, and 3D visualization of γ and γ' phases are presented in Fig. 10.

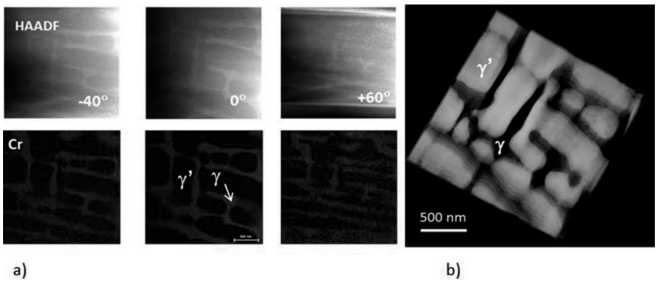

Fig. 10. Visualization of γ and γ' phases in CMSX-4 superalloy (region: T= 997°C, σ = 30 MPa) using STEM-EDX tomography method. a) HAADF-STEM and STEM-EDX elemental Cr map images at -40°, 0° and 60° tilt angle, selected from the registered tilt series, b) 3D visualization of γ and γ' phases

7. Summary

Various electron tomography methods (STEM-HAADF, STEM-EDX, EFTEM, FIB-SEM) were applied to investigation several materials for energy systems and aeronautics. In comparison to a conventional TEM, electron tomography methods permit to qualify complementary information about material microstructure and nanostructure. Microstructural features, such as morphology, size, and distribution of various precipitates and dispersoids, as well as porosity and grain size were visualizes and quantified in three dimensional space. Electron tomography methods are new promising tools for quantitative characterization of the spatial distribution of the particles in a solid material, complementary to conventional particle analysis methods, e.g. quantitative TEM metallography.

The Focused Ion Beam tomography has become an important tool for relatively fast and easy visualization and metrology of microstructural features in micro- and nanometer scale.

FIB-SEM tomography results of several commercial materials confirmed the ability of this method to get 3D reconstruction of the objects of 100 nm or even smaller, however selecting the SEM imaging method has a significant influence on the results of qualitative and quantitative assessment of the microstructure.

Three dimensional distribution of chemical elements was successfully studied in commercial CMSX-4 superalloy due to application of new STEM-EDX tomography and availability of most modern STEM-EDX system of 4 SDD detectors in probe Cs corrected TEM.

Received: 20 January 2013.

Acknowledgements

The financial support by the European Institute of Innovation and Technology, under the KIC InnoEnergy NewMat project (KIC NewMat, nr 7.7.110.7023) is gratefully acknowledged. The authors thank Mr A. Gruszczynski, MSc. (AGH-UST) for his assistance in the FIB-SEM investigation.

REFERENCES

[1] A. Kruk, B. Dubiel, W. Osuch, G. Cempura, A. Czyrska-Filemonowicz, Inżynieria Materiałowa **30**, 86 (2010).
[2] B. Dubiel, A. Kruk, E. Stępniowska, G. Cempura, D. Geiger, P. Formanek, J. Hernandez, P. Midgley, A. Czyrska-Filemonowicz, Journal of Microscopy **236**,149 (2009).
[3] J. Frank, Electron Tomography: Three-dimensional Imaging with the Transmission Electron Microscope, 2nd ed., Plenum Press, New York, (2007).
[4] P.A. Midgley, M. Weyland, Ultramicroscopy **96**, 413 (2003).
[5] R. Williams, D. Bhattacharyya, G.B. Viswanathan, R. Banerjee, H.L. Fraser, Microscopy and Microanalysis **10**, 1178 (2004).
[6] F. Lasagni, A. Lasagni, M. Engstler, H.P. Degischer, F. Mücklich, Advanced Engineering Materials **10**, 62 (2008).
[7] J. Orloff, M. Utlaut, L. Swanson, High Resolution Focused Ion Beam, Kluwer Academic Plenum Press 2003.
[8] L. Giannuzzi, F.A. Stevie, Introduction to Focused ion Beams, Springer 2005.
[9] J. Wosik, Evaluation of the long-term microstructural stability of selected Ni-base superalloys, PhD thesis, AGH Kraków 2002.
[10] S. Milc, A. Kruk, G. Cempura, H.J. Penkalla, C. Thomser, A. Czyrska-Filemonowicz, Physica Scripta **T145**, 1 (2011).
[11] W. Osuch, A. Kruk, G. Michta, A. Czyrska-Filemonowicz, Solid State Phenomena **186**, 41 (2012).
[12] A. Czyrska-Filemonowicz, B. Dubiel, A. Wasilkowska, Żaroodporne i żarowytrzymałe stopy ODS umocnione nanocząstkami tlenków (Heat resistant ODS alloys strengthened by oxide nanoparticles), Fotobit, (2004).
[13] B. Dubiel, A. Czyrska-Filemonowicz, Solid State Phenomena **186**, 139 (2012).